ELSEVIER

Contents lists available at ScienceDirect

# Journal of Crystal Growth

journal homepage: www.elsevier.com/locate/jcrysgro



# Formation mechanism of two-dimensional hexagonal silica on SiO<sub>2</sub>/Si substrate

Nuzhat Maisha <sup>a</sup>, Olugbenga Ogunbiyi <sup>b</sup>, Guanhui Gao <sup>c</sup>, Mingyuan Sun <sup>d</sup>, Alexander Puretzky <sup>e</sup>, Bo Li <sup>d</sup>, Yingchao Yang <sup>a,b,\*</sup>

- <sup>a</sup> Department of Mechanical Engineering, University of Maine, 75 Long Road, Orono, ME 04469, USA
- b Department of Mechanical and Aerospace Engineering, University of Missouri, 416 S. 6th Street, Columbia, MO 65211, USA
- Department of Materials Science and Nanoengineering, Rice University, 6100 Main Street, Houston, TX 77005, USA
- d Department of Mechanical Engineering, Villanova University, 800 E. Lancaster Ave. Villanova, PA 19085, USA
- <sup>e</sup> Center for Nanophase Materials Sciences, Oak Ridge National Laboratory, 1 Bethel Valley Road, Oak Ridge, TN 37830, USA

ARTICLE INFO

Communicated by Maria Hilse

#### ABSTRACT

Owing to their remarkable electronic properties, silica ultrathin films have been utilized as an insulating layer in nanoelectronics systems. Silica films have been epitaxially grown on different substrates using various synthesis methods. Among all fabrication approaches, chemical vapor deposition has long been an advanced method for synthesizing two-dimensional (2D) materials due to its ability to ensure precise stacking control and minimize contamination between layers. This study harnessed the potential of CVD to atomically fabricate thin layered 2D silica on a SiO<sub>2</sub>/Si substrate. Significantly, a unique combination of multiple transition metals and salt as the catalysts aided the formation of 2D silica for the first time. Salt is a crucial catalyst in promoting the evaporation of high-melting-point metal catalysts, resulting in hexagonal nucleation sites on the SiO<sub>2</sub>/Si wafer. By meticulously controlling growth parameters, a distinctive hexagonal structure was obtained. Correspondingly, this work delves into the growth mechanism of 2D silica, as evidenced by experiments involving salt alone and individual transition metals. Group VB transition metals played a prominent role in achieving the hexagonal structure compared to their group IVB counterparts. This research offers insight into the formation and growth mechanism of 2D silica, expanding the understanding of silica nanostructures.

#### 1. Introduction

Ever since the discovery of graphene in 2004, two-dimensional (2D) materials have gathered enormous attention from researchers and have been synthesized via different methods, such as chemical vapor deposition (CVD) [1], molecular beam epitaxy [2], liquid template corrosion [3], solid-state reaction followed by mechanical exfoliation. 2D materials can be categorized into insulators (e.g., hexagonal boron nitride (*h*-BN)), semiconductors (e.g., transition metal dichalcogenides (TMDs)), and supplementary semi-metals (e.g., graphene, black phosphorous) [1]. Their unique features and physical properties, compared to individual bulk counterparts, have shown a significant array of optical, mechanical, chemical, and electric phenomena, enabling a wide range of applications, including photodetectors [4], high-strength composites [5], advanced catalysts [6,7], field-effect transistors [8,9]. Beyond well-known 2D materials, silica, generally known as silicon dioxide (SiO<sub>2</sub>),

can also exist in a 2D form for electronics and catalysis [10-12]. Through direct or indirect synthesis, 2D silica may exist as a crystalline or amorphous structure (glass). For instance, a bilayer 2D silica was accidently synthesized during the growth of graphene on copper foils using CVD approach [13]. The formation mechanism was attributed to contaminant in the graphene growth furnace [10,13]. Compared to all previously reported 2D crystals, such as h-BN having a band gap up to 4.7 eV [14,15], theoretically, 2D silica has a substantial band gap of 7.69 eV [16], distinguishing it as an excellent dielectric material. Along with other properties, 2D silica has the bending rigidity value of  $.8 \pm 0.5$  eV, which advances it for potential applications in flexible electronics and strain engineering [12]. Moreover, 2D silica nanosheets were demonstrated as a suitable catalyst in ammonia synthesis [17] and the capturing of CO<sub>2</sub> [18]. Due to their high surface area, 2D silica nanosheets possess the potential to serve as effective support for the development of amine-based sorbents [18].

E-mail address: yingchao.yang@missouri.edu (Y. Yang).

<sup>\*</sup> Corresponding author.

Recently, several efforts have been made to fabricate ultrathin 2D silica on a wide range of metal substrates [19]. These works were accompanied with theoretical studies to understand the growth mechanism and the underlying defects in 2D silica [20,21]. Metals catalysts, including Pt, Mo, Ni, Pd, Co and Ru, can facilitate the formation of silica layers [22]. Among various methods to synthesize layered silica structures, in situ growth of hexagonally ordered crystalline silica layers was achieved with a thickness of approximately one nanometer on transition metal surfaces in an electron microscope [22]. The nucleation of monolayer and bilayer silica layers formed via solid-state growth, culminating in the establishment of a stationary cellular structure. A strong bonding was found between the metal surface and the silica layer. To further understand the silica-metal bonding and the origin of defects, density functional theory (DFT) calculations revealed that metals with strong oxygen adsorption were responsible for forming monolayer silica, whereas bilayers result from weaker oxygen adsorption [10,23]. In addition, the lateral growth between the silica nucleation on the metal surface was limited due to the planar defect presence at the intersections of the metal surface [24]. 2D silica nanosheets with a large thickness of 5-7 nm were also synthesized via the wet chemical method. The obtained silica exhibits mechanical robustness, smooth surface, and compact structures [25]. The lateral dimension of these nanosheets varied in tens of micrometers. During growth, the size of intermediate particles accounted for the obtained amorphous 2D silica nanosheets [18]. Researchers have also adopted several materials as sacrificial hard templates, such as graphene [26], peptides [27] and block copolymers [28] for the synthesis of silica nanosheets. Although this approach was widely used, it was compromised since several intermediate treatments were required to obtain the final product [18]. Hence, a feasible and user-friendly approach is of dire necessity to synthesize amorphous or crystalline 2D silica with a well-defined shape and structure for a wide range of applications.

CVD has been considered one of the most efficient techniques to fabricate 2D materials as it offers precise control over the stacking orientation and can avoid contamination among layers [29-31]. Although a significant number of 2D materials, such as graphene [32-34], TMDs (e.g., MoS<sub>2</sub>, [35-38] MoSe<sub>2</sub> [39]), heterostructures (e.g., WSe<sub>2</sub>/MoSe<sub>2</sub>) [40], h-BN, [41,42] with various morphologies have been synthesized via CVD previously, a hexagonal shaped and readily synthesizable 2D silica has not been reported yet. In this work, we successfully developed an approach to synthesize atomically thin layered 2D silica on a SiO<sub>2</sub>/Si substrate using CVD. A mixture of multiple transition metals and salt was employed as the active catalysts for the growth of these 2D silica nanosheets. The salt played a key role in promoting the evaporation of high melting-point metal powders with hexagonal closepacked crystal structures that were responsible for hexagonal nucleation sites on the SiO<sub>2</sub>/Si wafer. A unique hexagonal structure was achieved through precise control of the growth parameters. The growth mechanism was further investigated by performing several control experiments with salt alone and individual transition metals. Overall, the group VB metals played a significant role in promoting a more uniform hexagonal structure compared to the other transition metals from group IVB. This work provides valuable insight into the formation and growth mechanism of 2D silica.

# 2. Experimental section/Methods

#### 2.1. Materials

Hafnium (Hf, 99.6 % purity), Tantalum (Ta, 99.98 % purity), Niobium (Nb, 99.8 % purity), Zirconium (Zr, 99,8% purity), and Titanium (Ti, 99.5 % purity) metal powders, sodium chloride (NaCl,  $\geq$  99 % purity) and Sulfur (S,  $\geq$  99.5 % purity) were purchased from Alfa Aesar and used as precursors. The SiO<sub>2</sub>/Si wafer, with a thickness of 300 nm SiO<sub>2</sub> on the top was purchased from the University Wafer and used as substrate. Acetone (purity 99.5 %) and Isopropyl alcohol (IPA) were

supplied by Alfa Aesar and Fisher Scientific, respectively and used for cleaning the substrate.

# 2.2. Synthesis of hexagonal 2D silica

The hexagonal structured 2D silica sample was synthesized in a quartz tube with a diameter of 50 mm. The length of the furnace is about 36 cm. Ar was used as the carrier gas with a flow rate of 120 sccm (cubic centimeters per minute). An aluminum oxide boat with a dimension of  $8.5 \text{ cm} \times 1.8 \text{ cm} \times 1 \text{ cm}$  containing the precursor powders was placed at the center of the tube. A mixture of five transition metal powders consisting of Group IVB and Group VB elements, such as Hf, Nb, Ta, Ti, and Zr metal powders, along with NaCl salt, was used as the precursor. A SiO<sub>2</sub>/Si wafer was cleaned ultrasonically first for 10 min in acetone, followed by 7–8 min in IPA. The substrate was placed on the aluminum oxide boat with the polished surface facing down. Another aluminum oxide boat containing S was placed at the upstream of the tube furnace, where the temperature ranges between 150 and 200 °C. The distance between the S and precursor boat is approximately 16 cm. The furnace was heated with a ramp rate of 30 °C min<sup>-1</sup> to the growth temperature of 950 °C and held at this temperature for 30-35 min before cooling to room temperature naturally.

# 2.3. TEM sample preparation

TEM samples were prepared with a poly (methyl methacrylate) (PMMA)-assisted method with the assistance of acetone and isopropyl alcohol droplet. The  $\rm SiO_2/Si$  substrate with the hexagonal structure was cut into small squares of 5 mm  $\times$  5 mm according to the size of the TEM grid. Then, a layer of PMMA was coated on the substrate with a VIVTE spin coater (Model; vivo-lsc-pa). Subsequently, the substrate containing the sample was heated at 90  $^{\circ} \rm C$  on a hot plate for 1 min. The PMMA film containing the sample was etched using a sodium hydroxide (NaOH) solution purchased from Sigma Aldrich. Afterwards, a TEM grid was used to fish out 2D silica/PMMA and washed a couple of times. Finally, the specimen together with the TEM grid was gently floated onto acetone to etch off PMMA. After acetone evaporation, the TEM grid loaded with 2D silica is ready for TEM observation.

# 2.4. Characterization

The morphology and chemical composition of the synthesized 2D silica samples were characterized by optical microscopy (AmScope Microscope MX6R), scanning electron microscopy (AMRAY 1820 SEM), energy dispersive X-ray analysis (EDX, equipped with AMRAY 1820 SEM), and transmission electron microscopy (FEI, Titan Themis S/TEM). Raman spectroscopy was performed on Horiba Xplore Plus Raman microscope with 523 nm excitation. The atomic thickness of the as-grown 2D silica was measured by a Bruker Dimension Icon scanning probe microscope.

#### 3. Results and discussions

A combination of five transition metal powders consisting of elements from Group IVB (Hf, Ti, Zr) and Group VB (Nb, Ta), along with NaCl and chalcogen sulfur, was primarily employed as precursors to synthesize 2D high-entropy materials (HEMs). Generally, the growth of common 2D TMDs, such as  $MoS_2$ ,  $WS_2$  and  $NbS_2$ , can be typically achieved at a lower temperature from  $600\,^{\circ}\text{C}$  to  $850\,^{\circ}\text{C}$  [39]. However, the combination of these elements yielded crystals, but no all metals showed up at this temperature range. To ensure optimum evaporation of all high melting-point transition metal powders, the temperature was elevated to 950  $^{\circ}\text{C}$ . During the growth of HEMs, salt is expected to reduce the precursors' melting points and promote the overall reaction rate [39]. Interestingly, hexagonal 2D silica rather than 2D HEMs was obtained. A series of characterizations were carried out to understand the

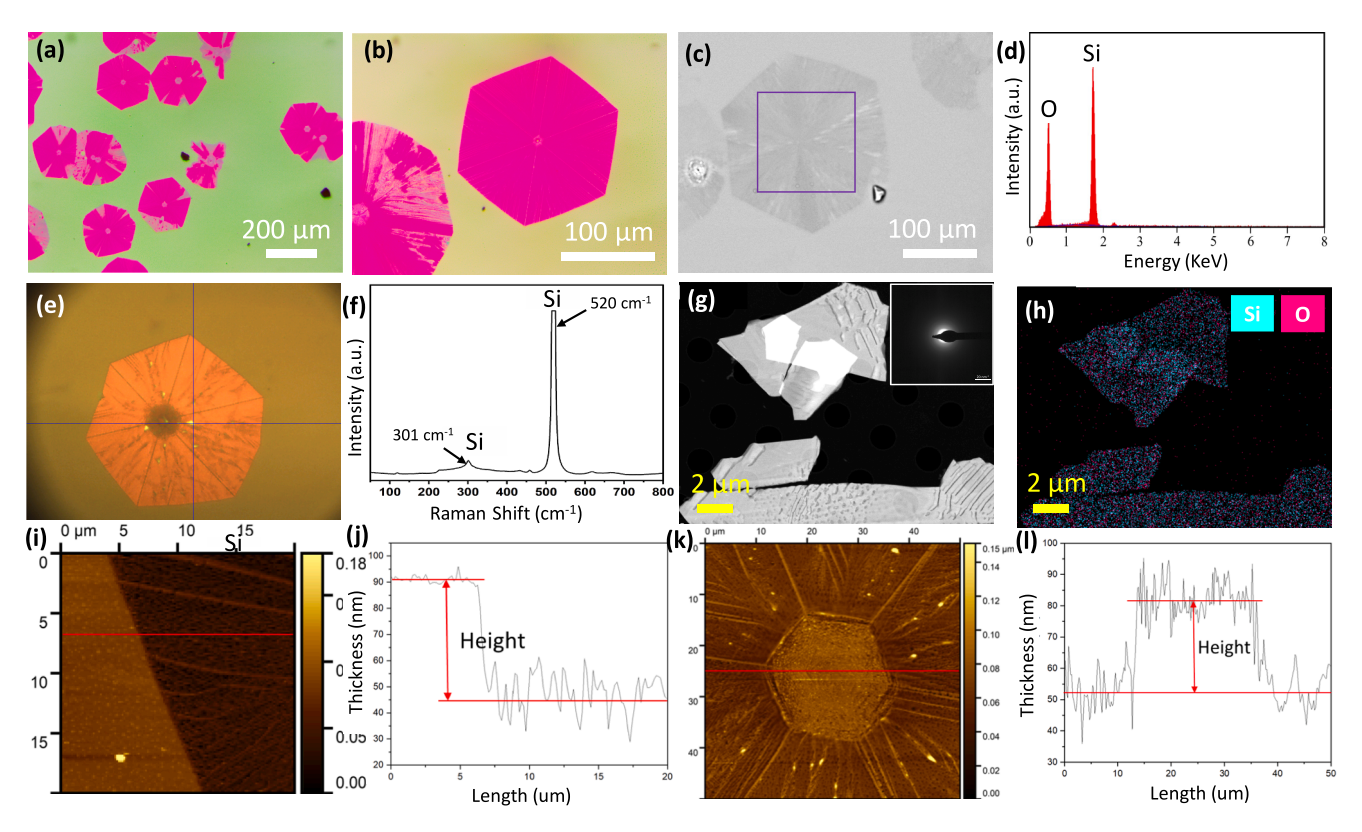


Fig. 1. Morphology and structure of the synthesized hexagonal 2D silica. (a,b) Optical images, (c) SEM image, (d) EDS spectrum from the squared area on the 2D silica in (c). (f) Raman spectrum of the 2D silica from the fine crosshair in (e). (g) TEM image of 2D silica with selected area diffraction (SAD) as inset. (h) EDS mapping indicating uniform distribution of Si and O. (i-l) AFM images and height profiles of the edge and the center of 2D hexagonal silica.

morphology and structure of the fabricated 2D silica.

Fig. 1(a) shows an optical image of 2D silica hexagons in high density. The size of the hexagon can be as large as  $\sim 200~\mu m$  . Unlike other TMDs with uniform morphology, the grown 2D silica hexagons have a great number of defects, such as cracks and boundaries. Occasionally, an individual hexagon has a uniform structure, as demonstrated in Fig. 1 (b). The hexagonal structures can also expand to form a continuous 2D film on the substrate. SEM imaging and EDS analyses were carried out to further visualize the defects and learn if there are any residual transition metal nucleation. Fig. 1(c) clearly shows a nonuniform texture with gaps between hexagonal flakes. From EDS analysis, both Si and O elements are found at an energy of 1.70 KeV and 0.52 KeV, respectively, with atomic percentages of 73 % (Si) and 27 % (O) (Fig. 1d). Regarding that the Si substrate is with 300 nm SiO<sub>2</sub> layer on the top and the EDS element signal can be from approximately 10 µm below the surface, such atomic percentages cannot be directly used to determine the atomic ratio of the grown silica layers. However, one can be sure is that no transition metals are found at the center and across the hexagonal structure. The observation supports the hypothesis that transition metals served as heterogeneous catalysts, aiding in the growth of the 2D silica hexagon without incorporating into the structure itself. Fig. 1(f) shows the Raman spectra taken from the fine crosshair on the hexagon in Fig. 1 (e). Two peaks at 520 cm<sup>-1</sup> and 301 cm<sup>-1</sup> revealed in Fig. 1(f) are the signals from the 2D silica, which matches the Raman peaks of the  $SiO_2$ / Si wafer reported previously [43].

To understand the atomic structure of the as-grown 2D silica and confirm the chemical composition, the high-angle annular dark field (HAADF) transmission electron microscope (TEM) imaging was performed and shown in Fig. 1(g). Defects shown as dotted lines are found in the sheet-like pieces of the hexagonal structure. The dotted lines on this image were also observed in the hexagonal structures of 2D silica in Fig. 1(e) and Fig. 1(e). Therefore, the thickness of the 2D silica is not flat locally. Confirmed by selected area diffraction (SAD) (Inset of Fig. 1(g)),

the obtained 2D silica is amorphous. The corresponding elemental EDS mapping shown in Fig. 1(h) reveals the uniform distribution of Si and O atoms represented by blue and pink colors, respectively, which confirms the formation of 2D silica in the synthesized hexagonal flake. The atomic percentages of Si and O atoms from the EDS spectrum are 30.03 % and 48.20 %, respectively, which indicates the atomic ratio of Si:O is about 1: 1.6 instead of 1:2. Therefore, the 2D silica consists of stable SiO2 and metastable SiO. Fig. 1(i-1) shows atomic force microscopy (AFM) images for morphology and thickness measurement of the synthesized 2D silica hexagon. Fig. 1(j) exhibits the height profile of the edge of the 2D silica hexagon obtained from Fig. 1(i), indicating that the obtained hexagonal structure has a uniform thickness in a large scale, and the thickness is approximately 45 nm. However, the alternative peaks and valleys suggest that the thickness is not uniform locally. The height profile in Fig. 1 (l), plotted from Fig. 1(k), reveals that the thickness at the center of the hexagon is 30 nm higher than that at the edge, which suggests a vapor-solid growth mechanism for this silica hexagon formation.

Therefore, high temperatures facilitate the formation of silica rather than TMDs, which agrees well with previous findings. For example, Si nanosheets were successfully synthesized on a Si substrate at 1,000 °C in the presence of silicon chloride (SiCl<sub>4</sub>) with a reaction time of 30 min [44]. Silica nanowires were also reported to grow at a temperature of  $900\sim1,\!100$   $^{\circ}\text{C},$  with Si and O atoms acting as catalysts. These atoms were produced from the oxidation reaction of silicon carbide (SiC) during the ablation process, leading to the formation of silica nanoparticles from silicon monoxide (SiO) and silicon oxide (SiO2) vapors [44]. As most transition metals effectively reduce the oxide layer on SiO<sub>2</sub>/Si by forming volatile suboxides through the surface reaction and deposition on the SiO2 surface, in this work, the catalytic mixture of transition metals at high temperatures may work to decompose surface SiO<sub>2</sub> on the substrate into Si and O atoms [45]. Once the Si-O-Si bond is broken, the Si atoms will follow the O atoms and react with each other, eventually forming a hexagonal structure of silica.

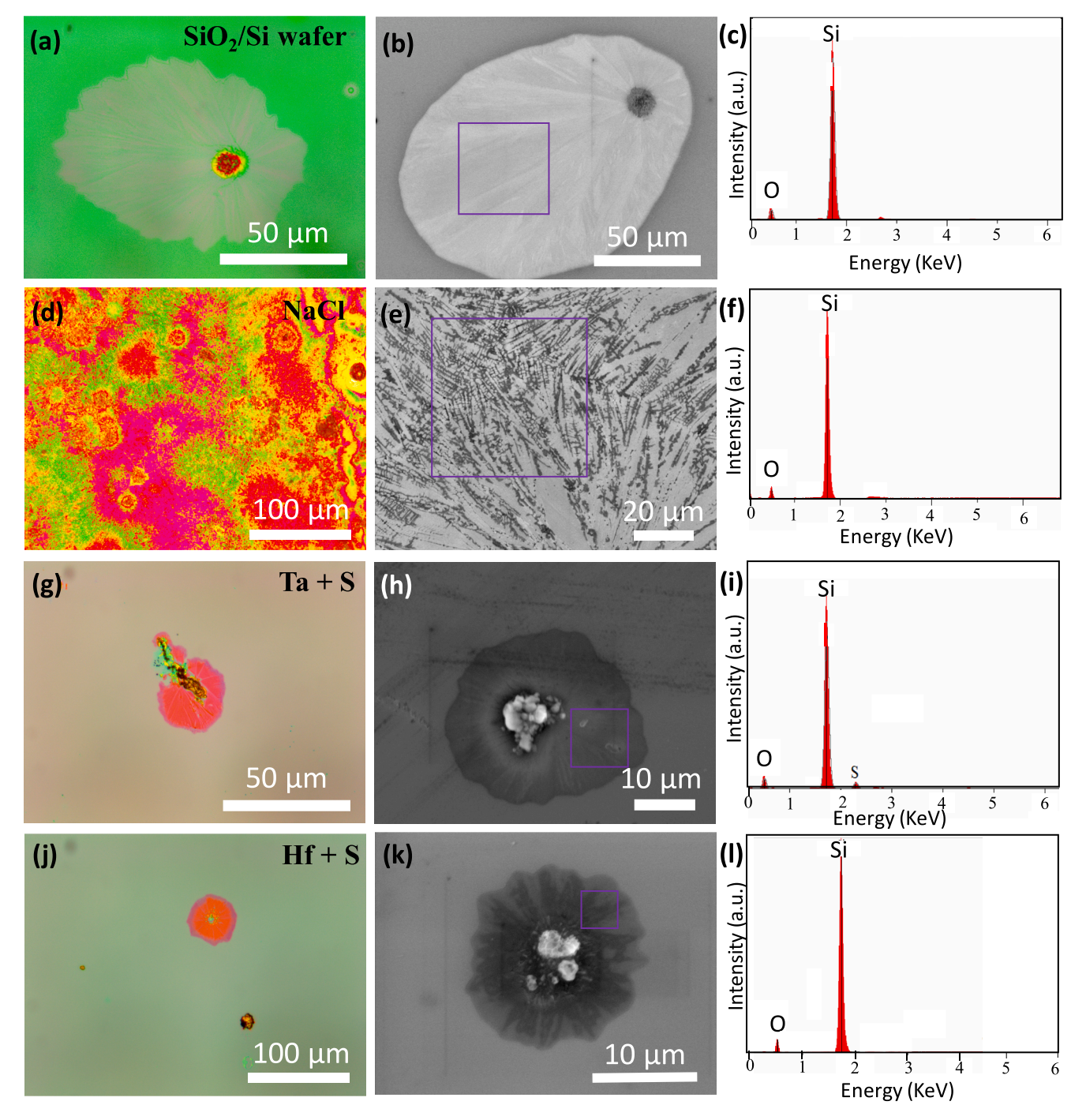


Fig. 2. Growth of 2D silica to learn the role of salt. (a) Optical and (b) SEM images of  $SiO_2/Si$  wafer treated at 950 °C without any precursor materials. (c) EDS spectrum from the squared area in (b). (d) Optical and (e) SEM images of obtained 2D silica with salt as the only precursor. (f) EDS spectrum from the squared area in (e). (g) Optical and (h) SEM images of obtained 2D silica with Ta and S as the only precursor. (i) EDS spectrum from the squared area in (h). (j) Optical and (k) SEM images of obtained 2D silica with Hf and S as the only precursor. (l) EDS spectrum from the squared area in (k).

As  $SiO_2/Si$  wafer has been widely used as a substrate to synthesize 2D materials, the growth mechanism of 2D silica should be well understood to avoid misidentifying the synthesized specimens by morphology only. A series of experiments was carefully conducted to learn the role of one parameter in each round. Fig. 2 focuses on the role of NaCl towards nucleation and growth of 2D silica. All other parameters were kept the same, including temperature (950 °C), growth time (30 min), and carrier gas (Ar). Fig. 2(a) and 2(b), respectively, show optical and SEM images of  $SiO_2/Si$  wafer treated at 950 °C without any precursors. A few areas are found with irregularly shaped structures, possibly due to residual

ethanol or acetone after washing following thermal treatment. Fig. 2(c) shows the EDS analysis of the irregular structure, confirming the presence of both Si and O on the  $SiO_2/Si$  wafer. The benchmark experiment suggests that the formation of hexagonal 2D silica does not result from the rearrangement of Si and O atoms in the substrate at a high temperature. After the control experiment, NaCl was placed into a crucible boat, where a piece of  $SiO_2/Si$  wafer was placed on the boat and over the NaCl. Fig. 2(d) demonstrates the macroscale pattern obtained after thermal treatment. The SEM image in Fig. 2(e) clearly shows needle-like structures formed on the  $SiO_2/Si$  surface. The different morphologies in

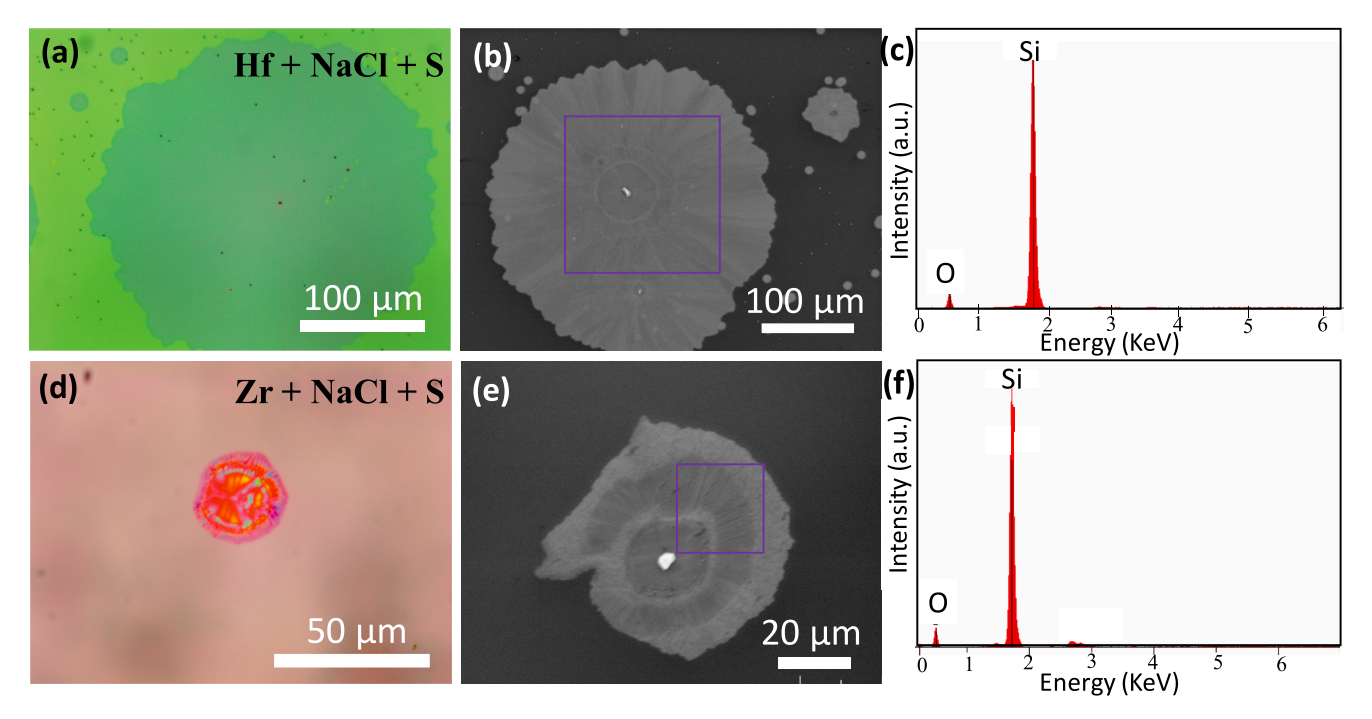


Fig. 3. Growth of 2D silica to learn the role of Group IVB metals. (a) Optical and (b) SEM images of obtained 2D silica with Hf, S and NaCl as the precursor. (c) EDS spectrum from the squared area in (b). (d) Optical and (e) SEM images of obtained 2D silica with Zr, S and NaCl as the precursor. (f) EDS spectrum from the squared area in (e).

Fig. 2(a)-2(d) indicate that a reaction between  $SiO_2/Si$  and NaCl happened. NaCl has a melting point of  $\sim 801$  °C, lower than the setpoint 950 °C. During thermal treatment, NaCl was in the state of melting, delivering vapor to the  $SiO_2/Si$  substrate and subsequently etching the substrate slightly. As a result, the pattern in Fig. 2(e) was formed. Fig. 2 (f) shows significant Si and O elements, as well as a very weak Cl peak at the energy of 2.6 eV. Although the morphology of  $SiO_2$  was impacted by

NaCl, the cubic structure of NaCl cannot lead to the formation of hexagonal silica.

The role of the transition metals in the absence of NaCl in forming 2D silica was further investigated. Fig. 2(g), 2(h), 2(j), and 2(k) demonstrate  $SiO_2$  morphology when Hf or Ta was used along with S as the precursor. Apparently, small structures were obtained. Compared to the hexagonal structures in Fig. 1(a) and 1(b), the structures are small and have an

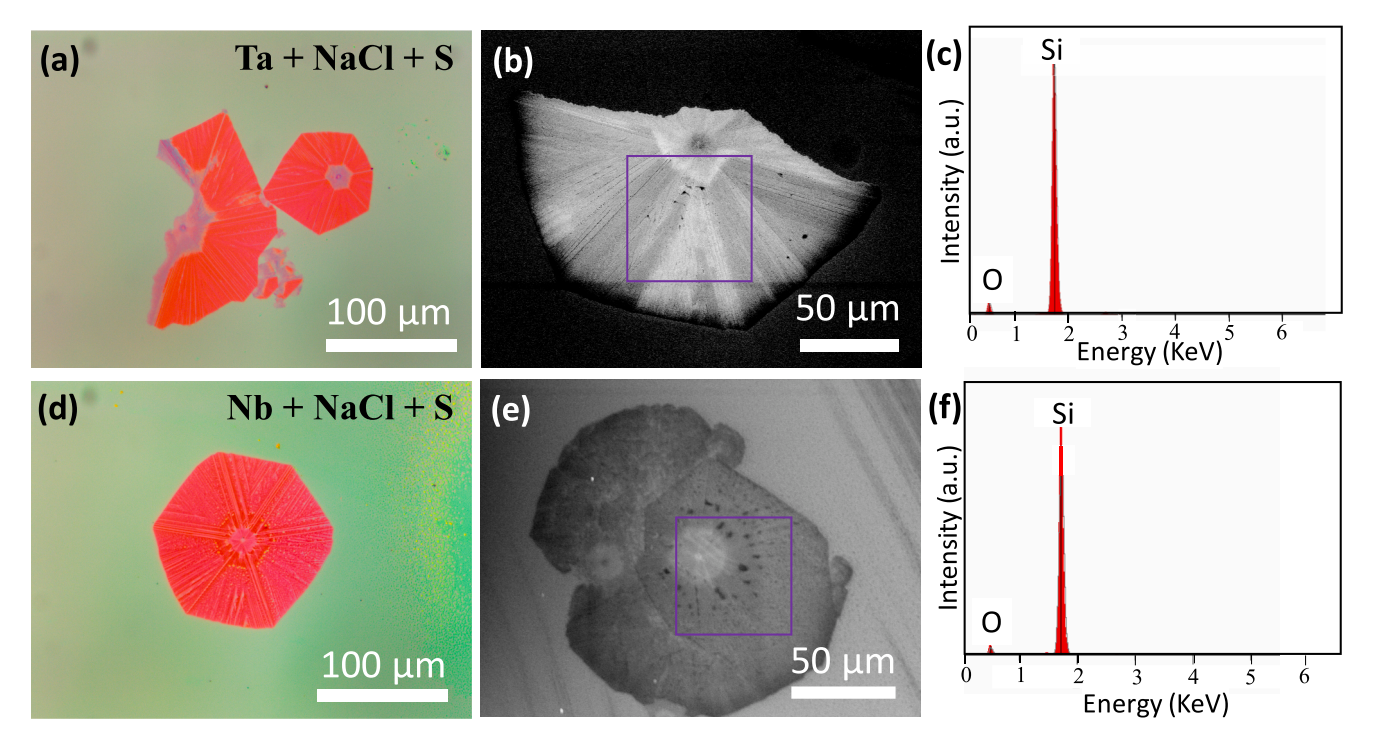
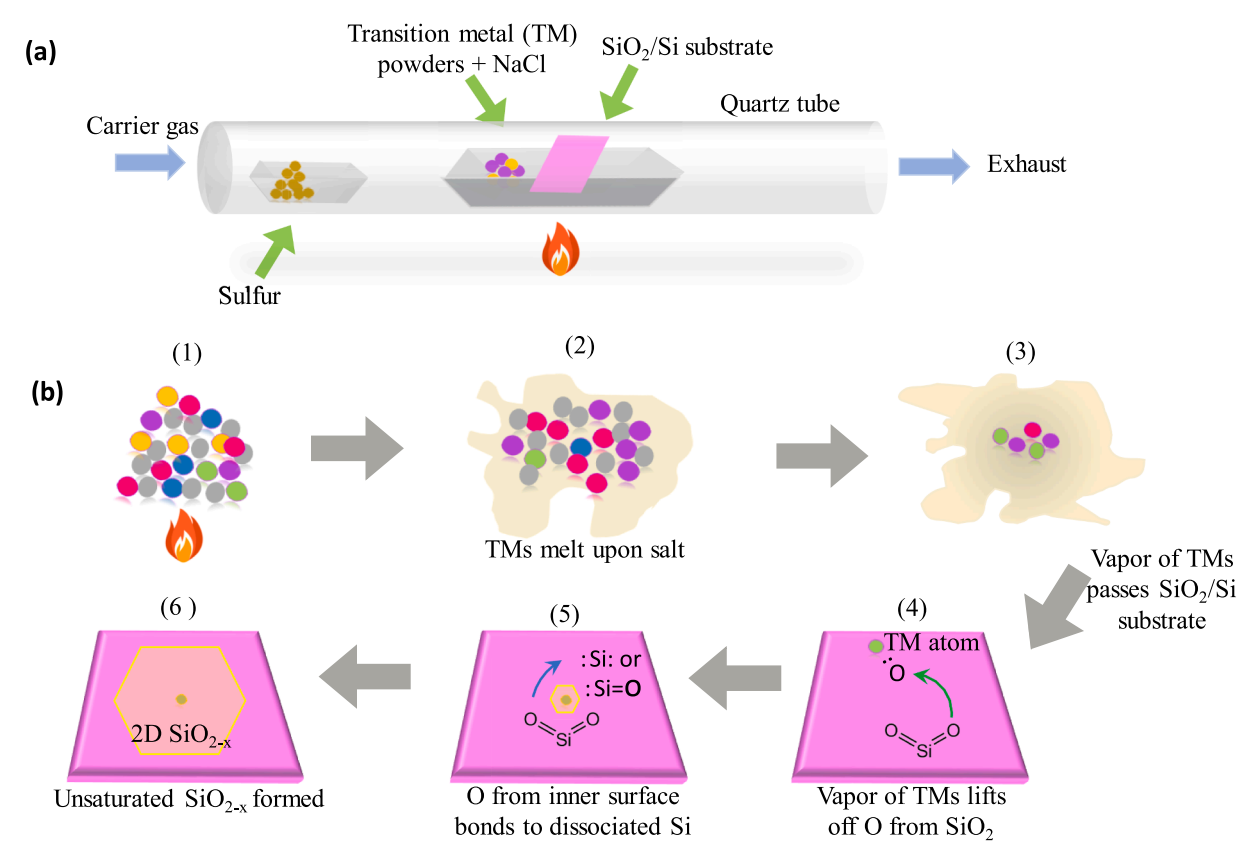


Fig. 4. Growth of 2D silica to learn the role of Group VB metals. (a) Optical and (b) SEM images of obtained 2D silica with Ta, S and NaCl as the precursor. (c) EDS spectrum from the squared area in (b). (d) Optical and (e) SEM images of obtained 2D silica with Nb, S and NaCl as the precursor. (f) EDS spectrum from the squared area in (e).



**Fig. 5.** Schematics for SiO<sub>2</sub> formation. (a) Illustration of the CVD synthesis setup. (b) Growth mechanism of 2D silica, where (B1)-(B3): salt (grey balls) reducing the melting point of transition metals (multicolored balls); (b4)-(b6): growth route of 2D silica with hexagonal nucleation sites resulting from the transition metals.

irregular shape. The small size may be due to the lack of Si and O sources during the growth. Fig. 2i shows the EDS spectrum of the red part in Fig. 2(g), indicating that the obtained specimen is  $\mathrm{SiO}_2$  but with trace amounts of residual sulfur. The EDS spectrum in Fig. 2(l) also confirms that the obtained structures predominantly consist of Si and O as well. This comparison collectively suggests that neither the substrate, salt nor the transition metals are solely responsible for the growth of unique 2D silica. A combination of transition metals and salt is required to achieve large and uniformly distributed 2D silica.

The transition metals used for the synthesis of HEMs can be categorized into two groups: Group IVB (Hf, Ti, Zr) and Group VB (Nb, Ta). Individual metal in each group was mixed with NaCl and sulfur. The mixture was used as a precursor to investigate the possibility of obtaining any 2D silica. Fig. 3(a) and 3(b) present the formation of an irregularly shaped large-size structure on the  $SiO_2/Si$  wafer where the transition metal in the precursor is Hf. Fig. 3(c) confirmed the chemical composition of Si and O. Similarly, an irregular structure is observed in Fig. 3(d) and 3(e) on the substrate when the transition metal Zr from the same group (IVB) was mixed with NaCl salt as the precursor. Fig. 3(f) demonstrates the elements of Si and O in the grown structure. Based on the morphology obtained from Hf and Za combined with S and NaCl, the Group IVB metals alone cannot help the formation of hexagonal silica.

After examining the effect of Group IVB transition metals on the growth of 2D silica, Group VB transition metals, including Ta and Nb, were added into precursors for the growth of silica. All other conditions were kept the same. Fig. 4(a) shows the optical image of a nearly hexagonal structure of 2D silica, where the precursor consists of a mixture of Ta, S, and NaCl. As the fabrication was carried out at 950 °C, the S vapor was predominantly exhausted without significant contribution to the growth of 2D silica. The SEM image in Fig. 4(b) also shows the obtained silica having the same needle-like structures found in Fig. 4(e). The EDS spectrum in Fig. 4(c), obtained from Fig. 4(b), shows both Si and O.

There is no residue of Ta and other elements in the structure. Similarly, when Nb was used as the precursor alongside NaCl, a complete hexagon with sharp edges and a uniformly distributed structure was observed (Fig. 4(d)). Only Si and O signals can be observed from Fig. 4(f). Therefore, Group VB transition metals are found to have a more pronounced effect on the formation of the hexagonal 2D silica compared to Group IVB transition metals.

Based on the comparison of the performed experiment and the observed relationship between morphologies and the used precursors, the growth mechanism of 2D silica is proposed and schematically presented in Fig. 5. Fig. 5(a) demonstrates the synthesis of hexagonal 2D silica flakes on a SiO<sub>2</sub>/Si substrate in a single-zone tube furnace. The high synthesis temperature, 950 °C, allows the formation of silica but not TMDs. Fig. 5(b1)-1(b3) schematically illustrate NaCl facilitating the melting of transition metals at temperature of 950 °C [4], which is much lower than the melting point of either transition metals in the precursor. In addition to reducing melting points, salt can also promote the overall reaction rates and enable formation of more transition metal vapors, which interacts with the SiO<sub>2</sub>/Si substrate facing down to the transition metal precursor. The catalytic transition metal vapor will lift off oxygen in the SiO<sub>2</sub> (Fig. 5(b4)) at such high temperature and then form volatile suboxides through the surface reaction, leaving the dissociated :Si: or :Si = O on the surface (Fig. 5(b5)). To minimize surface energy, the unsaturated :Si: and :Si = O further bond to O in silica around the reaction area and from deeper surface. Such chemical reaction results in the oxygen deficiency, which is confirmed by the atomic ratio approximately 1:1.6 between Si and O measured on the specimen in TEM. During the O dissociation and :Si: or :Si = O stabilization through rebonding to O, the structure is under reconfiguration, leaving a large amount to defects, such as missing pieces, boundaries in Fig. 1(c) and 1 (g). The hexagonal structures may originate from the selected transition metal atoms having a hexagonal close-packed crystal structure. When

oxygen atoms are extracted from the top surface of the  $SiO_2/Si$  substrate, the :Si: or :Si = O may also attach to the transition metal atoms. With the dissociation, bonding, and reconfiguration occurring, a hexagonal structure may form shown in Fig. 1(a). However, if the reconfiguration is not centered around the transition metals, the final silica shape may not be in hexagonal shape, e.g. those in Fig. 4(a).

#### 4. Conclusion

The synthesis of atomically thin layered 2D silica on a  $SiO_2/Si$  substrate using the CVD technique has been successfully performed. A unique hexagonal structure of 2D silica was achieved by employing a mixture of multiple transition metals and salt as catalysts. Salt plays a crucial role in promoting the evaporation of high melting-point metal powders, which facilitate the formation of nucleation sites on  $SiO_2/Si$  substrate. Several investigations were conducted to understand the growth mechanism, including experimenting with salt alone and individual transition metals. The group VB transition metals have a more significant impact in promoting a uniform hexagonal structure compared to the group IVB metals. Our work expands the understanding of silica nanostructures and provides valuable insight for researchers on utilizing 2D silica for various applications.

# CRediT authorship contribution statement

Nuzhat Maisha: Writing – original draft, Methodology, Investigation, Formal analysis, Data curation. Olugbenga Ogunbiyi: Writing – review & editing, Visualization, Methodology. Guanhui Gao: Writing – review & editing, Visualization, Validation. Mingyuan Sun: Formal analysis, Visualization. Alexander Puretzky: Resources, Validation, Writing – review & editing. Bo Li: Formal analysis, Validation, Visualization, Writing – review & editing. Yingchao Yang: Validation, Conceptualization, Writing – review & editing, Formal analysis, Funding acquisition, Investigation, Methodology, Project administration, Supervision.

#### Declaration of competing interest

The authors declare that they have no known competing financial interests or personal relationships that could have appeared to influence the work reported in this paper.

#### Data availability

Data will be made available on request.

# Acknowledgements

N.M. and Y.Y. acknowledge the support from the U.S. Department of Energy, Office of Basic Energy Sciences, under grant number DE-SC0021127. O.O. and Y.Y. gratefully acknowledge financial support by the U.S. National Science Foundation, Faculty Early Career Development Program (CAREER), under award number 2144196.

# References

- [1] V. Brar, A. Koltonow, J. Huang, ACS Photonics 4 (2017) 407-411.
- [2] M. Nakano, Y. Wang, Y. Kashiwabara, H. Matsuoka, Y. Iwasa, Nano Lett. 17 (2017) 5595–5599.

- [3] W. Yang, B. Li, Nanoscale 6 (2014) 2292-2298.
- [4] F. Koppens, T. Mueller, P. Avouris, C. Ferrari, M. Vitiello, M. Polini, Nat. Nanotechnol. 9 (2014) 780–793.
- [5] C. Androulidakis, K. Zhang, M. Robertson, S. Tawfick, 2D Mater. 5 (2018) 032005.
- [6] D. Voiry, H. Yamaguchi, J. Li, R. Silva, D. Alves, T. Fujita, M. Chen, T. Asefa, V. Shenoy, G. Eda, M. Chhowalla, Nat. Mater. 12 (2013) 850–855.
- [7] S. Zhao, G. Chen, G. Zhou, L. Yin, J. Veder, B. Johannessen, M. Saunders, S. Yang, R. De Marco, C. Liu, S. Jiang, Adv. Funct. Mater. 30 (2020) 1906157.
- [8] T. Roy, M. Tosun, J. Kang, A. Sachid, S. Desai, M. Hettick, C. Hu, A. Javey, ACS Nano 8 (2014) 6259–6264.
- [9] F. Gao, H. Yang, P. Hu, Small Methods 2 (2018) 1700384.
- [10] J. Zhong, H. Freund, Chem. Rev. 122 (2022) 11172-11246.
- [11] M. Ogawa, Langmuir 13 (1997) 1853-1855.
- [12] C. Buchner, S. Eder, T. Nesse, D. Kuhness, P. Schlexer, G. Pacchioni, J. Manson, M. Heyde, B. Holst, H. Freund, Phys. Rev. Lett. 120 (2018) 226101.
- [13] P. Huang, S. Kurasch, A. Srivastava, V. Skakalova, J. Kotakoski, A. Krasheninnikov, R. Hovden, Q. Mao, J. Meyer, J. Smet, D. Muller, Nano Lett. 12 (2012) 1081–1086.
- [14] J. Wang, F. Ma, W. Liang, R. Wang, M. Sun, Nanophotonics 6 (2017) 943–976.
- [15] G. Giovannetti, P. Khomyakov, G. Brocks, P. Kelly, J. Van Den Brink, Phys. Rev. b. 76 (2007) 073103.
- [16] Z. Gao, X. Dong, N. Li, J. Ren, Nano Lett. 17 (2017) 772-777.
- [17] H. Fan, J. Folke, Z. Liu, F. Girgsdies, R. Imlau, H. Ruland, S. Heumann, J. Granwehr, R. Eichel, R. Schlogl, E. Frei, ACS Appl, Mater. Interfaces 13 (2021) 30187.
- [18] B. Singh, V. Polshettiwar, Nanoscale 11 (2019) 5365-5376.
- [19] C. Buchner, M. Heyde, Prog. Surf. Sci. 92 (2017) 341-374.
- [20] M. Durandurdu, Phys. Rev. B 81 (2010) 174107.
- [21] T. Bjorkman, S. Kurasch, O. Lehtinen, J. Kotakoski, O. Yazyev, A. Srivastava, V. Skakalova, J. Smet, U. Kaiser, A. Krasheninnikov, Sci. Rep. 3 (2013) 3482.
- [22] F. Ben-Romdhane, T. Bjorkman, A. Krasheninnikov, F. Banhart, J. Phys. Chem. C 118 (2014) 21001–21005.
- [23] C. Buchner, L. Lichtenstein, S. Stuckenholz, M. Heyde, F. Ringleb, M. Sterrer, W. Kaden, L. Giordano, G. Pacchioni, H. Freund, J. Phys. Chem. C 118 (2014) 20959–20969.
- [24] F. Ben-Romdhane, T. Bjorkman, J. Rodriguez-Manzo, O. Cretu, A. Krasheninnikov, F. Banhart, ACS Nano 7 (2013) 5175–5180.
- [25] X. Wang, J. Xu, Q. Wang, A. Xu, Y. Zhai, J. Luo, Y. Jiang, N. He, Z. Wang, Small 13 (2017) 1603369.
- [26] Y. Xue, Y. Ye, F. Chen, H. Wang, C. Chen, Z. Xue, X. Zhou, X. Xie, Y. Mai, Chem. Commun. 52 (2016) 575–578.
- [27] H. Lutz, V. Jaeger, R. Berger, M. Bonn, J. Pfaendtner, T. Weidner, Adv. Mater. Interfaces 2 (2015) 1500282.
- [28] D. Yao, Y. Chen, R. Jin, J. Mater. Chem. B 3 (2015) 5786–5794.
- [29] W. Yang, G. Chen, Z. Shi, C. Liu, L. Zhang, G. Xie, M. Cheng, D. Wang, R. Yang, D. Shi, K. Watanabe, Nat. Mater. 12 (2013) 792–797.
- [30] Y. Gong, J. Lin, X. Wang, G. Shi, S. Lei, Z. Lin, X. Zou, G. Ye, R. Vajtai, B. Yakobson, H. Terrones, Nat. Mater. 13 (2014) 1135–1142.
- [31] Y. Zhang, Y. Yao, M. Sendeku, L. Yin, X. Zhan, F. Wang, Z. Wang, J. He, Adv. Mater. 31 (2019) 901694.
- [32] A. Reina, X. Jia, J. Ho, D. Nezich, H. Son, V. Bulovic, M. Dresselhaus, J. Kong, Nano Lett. 9 (2009) 30–35.
- [33] A. Pollard, R. Nair, S. Sabki, C. Staddon, L. Perdigao, C. Hsu, J. Garfitt, S. Gangopadhyay, H. Gleeson, A. Geim, P. Beton, J. Phys. Chem. C 113 (2009) 16565–16567.
- [34] X. Li, W. Cai, J. An, S. Kim, J. Nah, D. Yang, R. Piner, A. Velamakanni, I. Jung, E. Tutuc, S. Banerjee, Sci. 324 (2009) 1312–1314.
- [35] Y. Lee, X. Zhang, W. Zhang, M. Chang, C. Lin, K. Chang, Y. Yu, J. Wang, C. Chang, L. Li, T. Lin, Adv. Mater. 24 (2012) 2320–2325.
- [36] B. Liu, L. Chen, G. Liu, A. Abbas, M. Fathi, C. Zhou, ACS Nano 8 (2014) 5304–5314.
- [37] S. Najmaei, Z. Liu, W. Zhou, X. Zou, G. Shi, S. Lei, B. Yakobson, J. Idrobo, P. Ajayan, J. Lou, Nat. Mater. 12 (2013) 754–759.
- [38] M. Laskar, L. Ma, S. Kannappan, P. SungPark, S. Krishnamoorthy, D. Nath, W. Lu, Y. Wu, S. Rajan, Appl. Phys. Lett. 102 (2013) 252108.
- [39] J. Zhou, J. Lin, X. Huang, Y. Zhou, Y. Chen, J. Xia, H. Wang, Y. Xie, H. Yu, J. Lei, D. Wu, Nature 556 (2018) 355–359.
- [40] Y. Gong, S. Lei, G. Ye, B. Li, Y. He, K. Keyshar, X. Zhang, Q. Wang, J. Lou, Z. Liu, R. Vajtai, Nano Lett. 15 (2015) 6135–6141.
- [41] Y. Shi, C. Hamsen, X. Jia, K. Kim, A. Reina, M. Hofmann, A. Hsu, K. Zhang, H. Li, Z. Juang, M. Dresselhaus, Nano Lett. 10 (2010) 4134–4139.
- [42] L. Song, L. Ci, H. Lu, P. Sorokin, C. Jin, J. Ni, A. Kvashnin, D. Kvashnin, J. Lou, B. Yakobson, P. Ajayan, Nano Lett. 10 (2010) 3209–3215.
- [43] W. Lee, Y. Chang, Coatings 8 (2018) 431.
- [44] U. Kim, I. Kim, Y. Park, K. Lee, S. Yim, J. Park, H. Ahn, S. Park, H. Choi, ACS Nano 5 (2011) 2176–2181.
- [45] M. Liehr, H. Dallaporta, J. Lewis, Appl. Phys. Lett. 53 (1988) 589–591.